

Chukwu, Richard ; Mugisa, John ; Brogioli, Dorianio ; La Mantia, Fabio



Dynamic Impedance Spectroscopy: Fitting Multivariate Impedance Spectra using B-Spline Basis

Conference paper as: peer-reviewed accepted version (Postprint)

DOI of this document* (secondary publication): <https://doi.org/10.26092/elib/3665>

Publication date of this document: 14/02/2025

* for better findability or for reliable citation

Recommended Citation (primary publication/Version of Record) incl. DOI:

R. Chukwu, J. Mugisa, D. Brogioli and F. La Mantia, "Dynamic Impedance Spectroscopy: Fitting Multivariate Impedance Spectra using B-Spline Basis," 2023 International Workshop on Impedance Spectroscopy (IWIS), Chemnitz, Germany, 2023, pp. 28-35, doi: 10.1109/IWIS61214.2023.10302759.

Please note that the version of this document may differ from the final published version (Version of Record/primary publication) in terms of copy-editing, pagination, publication date and DOI. Please cite the version that you actually used. Before citing, you are also advised to check the publisher's website for any subsequent corrections or retractions (see also <https://retractionwatch.com/>).

© 2023 IEEE. Personal use of this material is permitted. Permission from IEEE must be obtained for all other uses, in any current or future media, including reprinting/republishing this material for advertising or promotional purposes, creating new collective works, for resale or redistribution to servers or lists, or reuse of any copyrighted component of this work in other works.

This document is made available with all rights reserved.

Take down policy

If you believe that this document or any material on this site infringes copyright, please contact publizieren@suub.uni-bremen.de with full details and we will remove access to the material.

Dynamic Impedance Spectroscopy: Fitting Multivariate Impedance Spectra using B-Spline Basis

Richard Chukwu

Energiespeicher- und Energiewandlersysteme
Universität Bremen
Bremen, Germany
rchukwu@uni-bremen.de

John Mugisa

Energiespeicher- und Energiewandlersysteme
Universität Bremen
Bremen, Germany
mugisa@uni-bremen.de

Doriano Brogioli

Energiespeicher- und Energiewandlersysteme
Universität Bremen
Bremen, Germany
brogioli@uni-bremen.de

Fabio La Mantia

Energiespeicher- und Energiewandlersysteme
Universität Bremen
Bremen, Germany
lamantia@uni-bremen.de

Abstract—Classical approaches to modelling dynamic or multivariate impedance spectroscopy data rely on either fitting individual spectra using an iterative procedure or using a joint least-squares analysis combined with partial prior knowledge of the model as a function of parameters which show a dependence on a control variable such as voltage or time. However, these approaches often fail to provide accurate results due to their sensitivity to the initial guess of the model parameters and the lack of an adaptive modelling approach. We address these limitations by introducing an approach that combines the parametric modelling of single spectra and use cubic B-splines to introduce the dependence of such parameters on the control variable. We illustrate our method by analyzing a set of 50 spectra obtained from dynamic impedance studies of electron transfer involving a redox couple in solution. We further demonstrate that the spline-based method is less sensitive to initial guesses, outperforms classical fitting methods in preserving the model parameters' dependence on the control variable and yields a significantly lower weighted residual mean square value compared to classical approaches.

Index Terms—dynamic impedance spectroscopy, cubic splines, fitting, multivariate

I. INTRODUCTION

Electrochemical impedance spectroscopy (EIS) is an analytical technique that allows us to gain a fundamental understanding of the kinetics and transport properties of an electrochemical system. EIS works by perturbing the electrochemical system under test with a low amplitude ($\leq 5 - 10$ mV) sinusoidal signal (single sine) or a multisine signal, either in voltage or current, and observing the response in current or voltage, respectively [1]. Multivariate impedance measurements arise either from taking static measurements (single impedance

measurements taken over several frequencies of interest) as a function of some control variable such as potential [2], temperature [3], and state of charge [4], to mention a few or by taking dynamic impedance measurements obtained via multifrequency analysis (DMFA) [5] or some other technique [6]. This usually results in a sequence of varying spectra. Compared to a single static impedance measurement, a sequence of impedance measurements can offer more thorough and useful information. Furthermore, since the impedance is measured over time, it is possible to access dynamic features of the electrochemical system, including relaxation times and response times and the detection of temporal patterns. For instance, the dependence of the rate constant on the potential can be observed by taking several measurements at different potentials. Furthermore, EIS measurements of batteries recorded under varying conditions of health, temperature, and state of charge can be used to build predictive models for the state of health [7].

In order to extract kinetic information about the system from the obtained spectra, it is common to use equivalent circuit models (ECM). Equivalent circuit models comprise a finite set of passive elements such as resistors, capacitors and inductors. They may also contain generalised impedance elements such as the Warburg and Gerischer elements [8]. These equivalent circuit models serve as simplistic representations or analogues of the electrochemical system. In addition, generalised mathematical models such as rational polynomials with coefficients can be used to characterise the electrochemical system [9]. The process of fitting an equivalent circuit involves regression of the chosen model to the experimentally obtained impedance spectra.

The process is relatively straightforward for fitting single spectra as obtained from static impedance measurements. The

This work was supported by the European Research Council (ERC) under the European Union's Horizon 2020 research and innovation programme (grant agreement number 772579).

most common approach uses complex non-linear least squares. While this method works relatively well, it can be sensitive to the choice of initial guess and sometimes fail to converge. Several techniques have been developed to work around this issue, such as genetic algorithms [10] and partial impedance circuits [11] for automatic parameter identification. To avoid convergence issues arising from parameters going off-limits and inaccuracies resulting from calculating the Jacobian via finite differences, Mark Zic et al. [12] used a strategy that involved computing the Jacobian symbolically. They also incorporated the use of limits to keep the parameters within bounds during optimization. However, analytic derivatives are not always available especially when the equivalent circuit model/impedance function becomes more complex – hence the need to rely on alternative methods of tackling the issue of poor convergence.

The situation is slightly different for multivariate impedance fitting since a second dimension in addition to the frequency variable is introduced. Nevertheless, there are different approaches to fitting such types of impedance data. One procedure is using "fit from previous" which uses the optimal parameters from a fit of previous spectra as the initial guess for subsequent spectra in an iterative manner. This method has an inherent disadvantage: when the parameter values of previous spectra go off limits, the fit worsens in the subsequent spectra. Dygas et al. [13] presented a two-step joint least-squares analysis (as implemented in their MULTFIS program) where an ECM is first regressed on individual spectra using a least-squares fit and then the dependence of the model parameters is evaluated in a second step by imposing a functional form of the dependence of the parameters on the control variable. Their method was restricted to modelling temperature dependence and used the slow derivative-free simplex algorithm. Another limitation was the potential for uncertainty arising from fit errors made in the first step propagating into the second step.

Alberto Battistel et al. [14] proposed a procedure for fitting data obtained from DMFA. This method did not impose a functional form of the dependence of the parameters on any control variable. Instead, they proposed the minimization of a custom cost function that combined the classical non-linear fit (of all the spectra) and an additional term, which is the squared norm of the second derivative of the parameters with respect to the impedance index. The latter is a measure of the local smoothness of the parameters. A vector of smoothing factors was used as a penalty which controlled the trade-off between minimizing the chi-square and how smoothly the parameters vary from one spectra to the other. As the smoothing factor increases so does the smoothness of the parameter curves. In other words, the sum of the chi-square and the concavity of the parameters was minimized. This method is less sensitive to initial values and could actually be used to obtain starting parameters for subsequent fit. Also, this method allowed the parameters to vary smoothly between successive spectra. Nevertheless, choosing the appropriate value of the smoothing factor required cross-validation, which can be time-consuming.

This study proposes a new approach. We give a parametric

model for the single spectra, accounting for the frequency dependence of the impedance, and we model the dependence of the parameters with time as the control/indexing variable using B-splines of degree three (cubic). Using 50 sets of experimental impedance data obtained from the negative scan of dynamic impedance studies on redox couple in solution, we compare the batch fitting mode of the open-source impedance fitting python package Impedancepy [15] (later referred to as classical-fitting) with the spline-based approach (later referred to as spline fitting). We show that the spline-based method produces more accurate fits, is less dependent on the choice of starting parameters and preserves the smooth variation of the parameters.

II. DESCRIPTION OF THE METHOD

A. B-splines

B-splines are piecewise polynomial curves defined by their degree p , order $l = p + 1$, and their knots. The degree is equivalent to the degree of the polynomial. The knots are the elements of the knot vector $x = \{x_n\}$ and represent specific points in the domain of the B-spline where two polynomials join. The knot vector is defined such that $x_n \leq x_{n+1}$ for all $n = 0, 1, \dots, N - 1$. Two exterior knots define the overall domain of the regression. The piecewise polynomial between a pair of adjacent knots is of degree p , where p is one less than the order of the B-spline. A B-spline of order l is characterized by continuous m th derivatives for $m = 0, \dots, l - 2$. This definition imposes smoothness constraints on the piecewise polynomials. For instance, a cubic B-spline with $l = 4$ has continuous zeroth, first and second derivatives. B-splines are represented by employing a collection of basis functions and coefficients for simplicity and computational efficiency.

The set of $N - p + 1$ B-spline basis functions $\{B_{n,p}\}_{n=0}^{N-p}$ are defined by De-Boor [16] recurrence relations for every $n = 0, 1, \dots, N - p$ as follows:

For $p = 0$:

$$B_{n,0}(t) = \begin{cases} 1 & : x_n \leq t < x_{n+1} \\ 0 & : \text{otherwise} \end{cases}. \quad (1)$$

And for $p > 1$:

$$B_{n,p}(t) = \left(\frac{t - x_n}{x_{n+p} - x_n} \right) B_{n,p-1}(t) + \left(\frac{x_{n+p+1} - t}{x_{n+p+1} - x_{n+1}} \right) B_{n+1,p-1}(t) \quad (2)$$

where $B_{n,p}(t)$ is the B-spline, n is the index of the control point, p is the order of the B-spline t is the parameter value, and x_n represents the n th knot value. Fig 1 shows the cubic B-Spline basis functions with 13 uniformly spaced knots as (dashed lines) and the spline (solid line) is represented as a superposition of the basis functions before the minimisation of the spline coefficients.

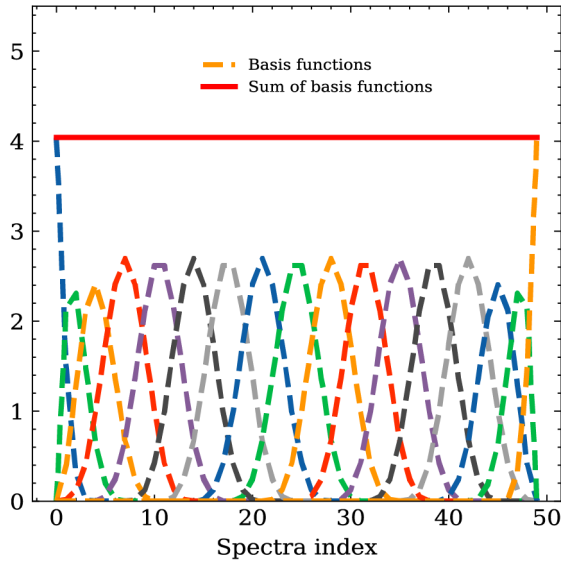


Fig. 1. Plot of the B-spline basis (degree=three, 13 knots). The dotted lines represent the basis functions while the thick lines represent the spline itself represented as a superposition of the basis functions before minimisation

B. Choosing the optimal number of knots

Selecting the right number of knots is crucial to the performance of B-splines. A large number of knots can result in overfitting, while insufficient knots can lead to underfitting. Since we chose a uniform spacing for the knots in this study, the spline's complexity is characterised only by the number of knots. Thus the optimal number of knots corresponds to that with the minimum value of the Akaike information criterion (AIC) [22]:

$$AIC = -2 \ln \hat{L} + 2(dim\hat{\theta})K \quad (3)$$

The first term in (3) contains the log-likelihood estimator which estimates, with some bias, the difference between the true distribution and the best model within a specific parameter space, $dim\hat{\theta}$ is the number of parameters and K is the number of knots. The second term on the right represents the effective model dimension and adjusts for bias [23]. The AIC as modified for complex impedance data for the case of modulus weighting by Ingdal and Harrington [24] was used in place of the original formula.

Another measure is the Akaike weight, which is between 0 and 1. It gives the probability that the model with the minimum AIC is the "best" among a number of candidate models. The Akaike weight W_i is defined as:

$$W_i = \frac{\exp(-\Delta_i/2)}{\sum_j \exp(-\Delta_j/2)} \quad (4)$$

where $\Delta_i = AIC_i - \min(AIC)$. Fig. 2 shows the Akaike weight plotted as a function of the number of knots for the fit carried out on the experimental data. The optimal number of knots can be seen to be 13 and this value corresponds to

the model with the highest probability given in terms of the Akaike weights. This value was used further in the analysis.

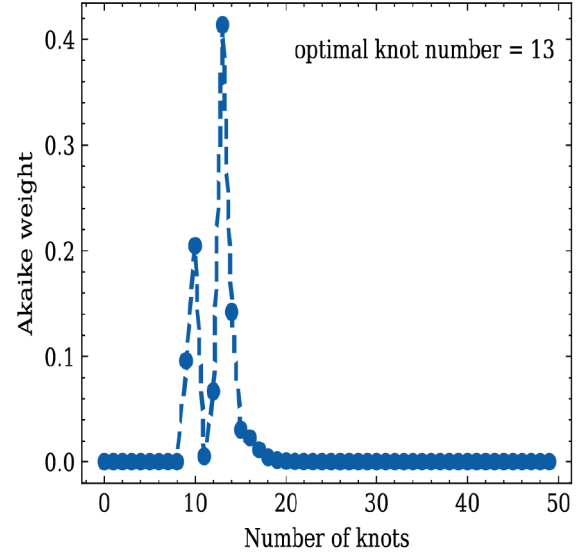


Fig. 2. Example of a figure caption.

C. Equivalent circuit models and starting parameters

Fig. 3 shows the equivalent circuit model used in this study. It is a modified Randles Circuit with the description of the component elements given below:

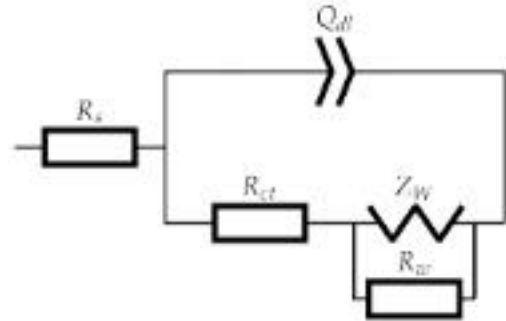


Fig. 3. Schematic representation of the equivalent circuit (modified Randles circuit) used.

- R_s represents the uncompensated solution resistance.
- Q_{dl} represents a constant phase element (CPE) which is used to describe the double layer.
- R_{ct} is the charge transfer resistance.
- Z_w represents the planar infinite Warburg element.
- R_w accounts for the dynamic effect on the impedance. the value of R_w could also be negative.

The starting parameter values and bounds are given in Table 1.

D. Model regression

We model the single impedance spectra with a function $Z_{\theta_n}(\omega)$. We attribute the variation of the spectra as a function

TABLE I
STARTING PARAMETER VALUES AND BOUNDS USED IN THE FIT

-	R_s (Ωm^2)	Q_{dl} ($Ss^n m^{-2}$)	n (-)	R_{ct} (Ωm^2)	W_{ct} ($\Omega s^{-0.5} m^2$)	R_w (Ωm^2)
Starting values	1.0e-2	3.0e-06	0.93	1.1e+04	4.7e05	1.3e06
Lower bounds	1.0e-15	1.0e-9	0.1	1.0e-15	1.0e-15	1.0e-15
Upper bounds	1.0e15	1.0e2	1.0	1.0e15	1.0e15	1.0e15

of the control parameter t to the variation of the parameters θ_d on t , thus the overall fitting function is $Z_{\theta_d(t)}(\omega)$. The goal is to obtain the time-varying parameters of the impedance model θ_d on t using B-splines, thus we model the time dependence as a superposition of spline basis functions $B_{n,p}(t)$:

$$\theta_d(t) = \sum_{n=0}^N C B_{n,p}(t) \quad (5)$$

where $\theta_d(t)$ represents the parameters of the model at time t , C is a matrix of coefficients, the rows of which have the same length as the number of parameters in the model and the columns have the same length as the number of basis functions. $B_{n,p}(t)$ is a matrix. The rows of this matrix represent time steps, and the columns correspond to the basis functions. Thus the optimal set of spline coefficients \hat{C} is defined such that:

$$\hat{C} = \underset{C}{\operatorname{argmin}} L(C) \quad (6)$$

where $L(C)$ represents the total cost function given by (7), minimized over all possible coefficients C .

$$L(\hat{C}) = \sum_{i=1}^T \chi_i^2 \quad (7)$$

The term χ_i^2 on the right hand side of (7) is the scaled version of the chi-square represented as:

$$\chi_i^2 = \sum_i^{N_f} w_i \left\{ Z_{\operatorname{Re},i} - \hat{Z}_{\operatorname{Re},i}[\theta_d(t)] \right\}^2 + \sum_i^{N_f} \left\{ Z_{\operatorname{Im},i} - \hat{Z}_{\operatorname{Im},i}[\theta_d(t)] \right\}^2 \quad (8)$$

where N_f , Z_i , \hat{Z}_i , w_i , θ_d , Re and Im represent the number of data points (frequencies measured), the i th value of the experimental impedance, the i th value of the calculated impedance, the weight associated with the i th frequency, the ECM parameters, real and imaginary respectively. We used modulus weighting for the fit. The `bs` function of Patsy's `dmatrix` [17] module was utilized to create the entire matrix of basis functions. Python's JAX library [18] was used to implement the minimization function, which allows for accurate computation of gradients through automatic differentiation, resulting in better convergence and eliminating inaccuracies associated with numerical finite differences. The spline fitting was done using JaxOpt's [19] `ScipyMinimize` module, with

the TNC method. The bounds were used to transform the parameters from linear to log scales, effectively shrinking the algorithm search space. We used the `CustomCircuit` module of `Impedancepy` [15] for the classical-fitting. The fitting algorithm used in `Impedancepy` [15] is based on Scipy's least-squares optimization module [20]. It is important to mention that with bounds provided, `Impedancepy` [15] uses the trust region reflective method of least-squares. Fig 4 depicts graphically the cubic B-Spline basis functions with 13 uniformly spaced knots (dashed line) and the spline (continuous line) after minimisation. The spline represents the parameter as it varies with time.

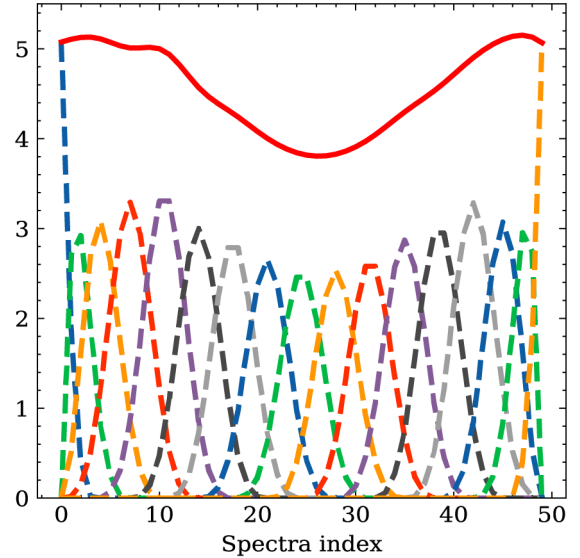


Fig. 4. Plot of the B-spline basis (degree=three, 13 knots). The dashed lines represent the basis functions while the solid line represents the spline itself represented as a superposition of the basis functions after minimisation

III. RESULTS AND DISCUSSION

Details on how the data was obtained have been given elsewhere [21] and will not be described here. The results of the fitting process for the approaches considered are shown in the Nyquist plots (Fig. 5). Only selected indexes are shown due to space constraints. Notice that the classical-fitting approach fails to fit the impedance at certain indexes. For instance, the fit at index 30 can be seen to be clearly off. On the other hand, the fitted results for the spline-fitting agree well visually with the experimental data over all the indexes shown. This fact suggests that the spline method is less sensitive to the choice of starting parameters.

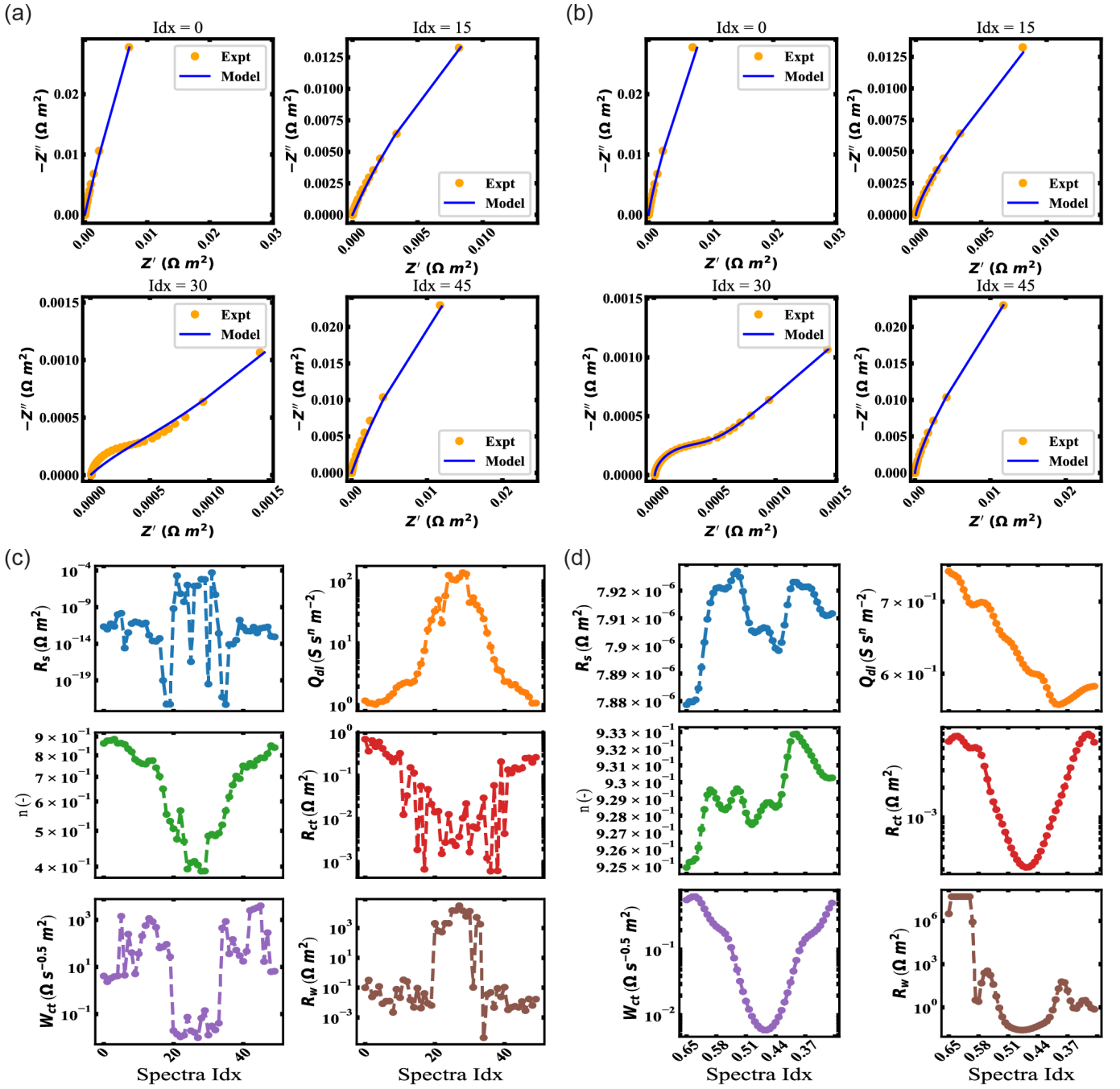


Fig. 5. Nyquist plots showing the experimental data and the model for the results obtained from (a) classical-fitting and (b) spline-fitting and the plot of fit parameters as a function of time (shown here as the spectra index) for the (c) classical-fitting and (d) spline-fitting.

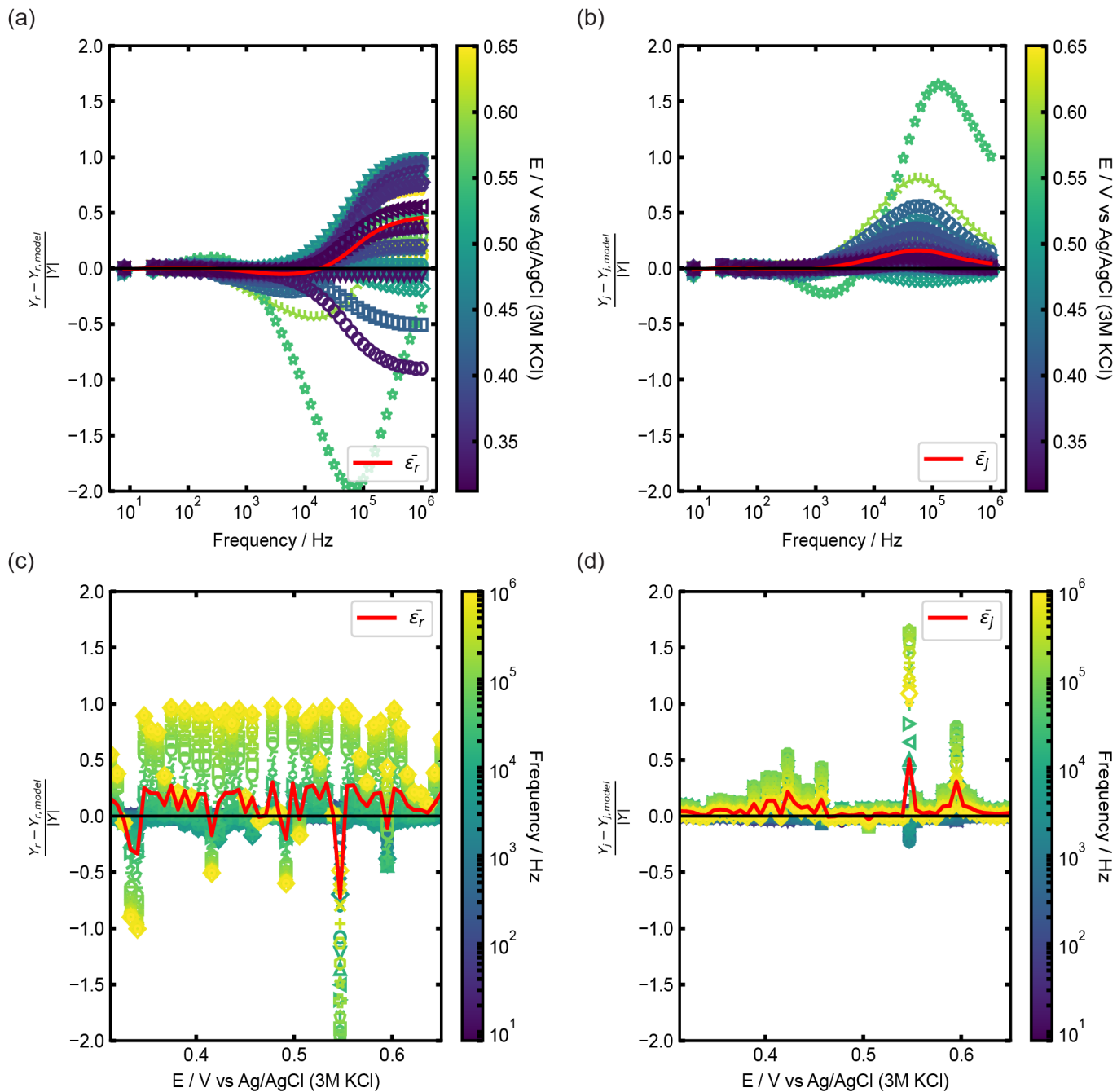


Fig. 6. Residual errors for the classical-fitting plotted as a function of frequency for the (a) real and (b) imaginary parts and as a function of voltage for the (a) real and (b) imaginary parts. The red line represents the mean of the values.

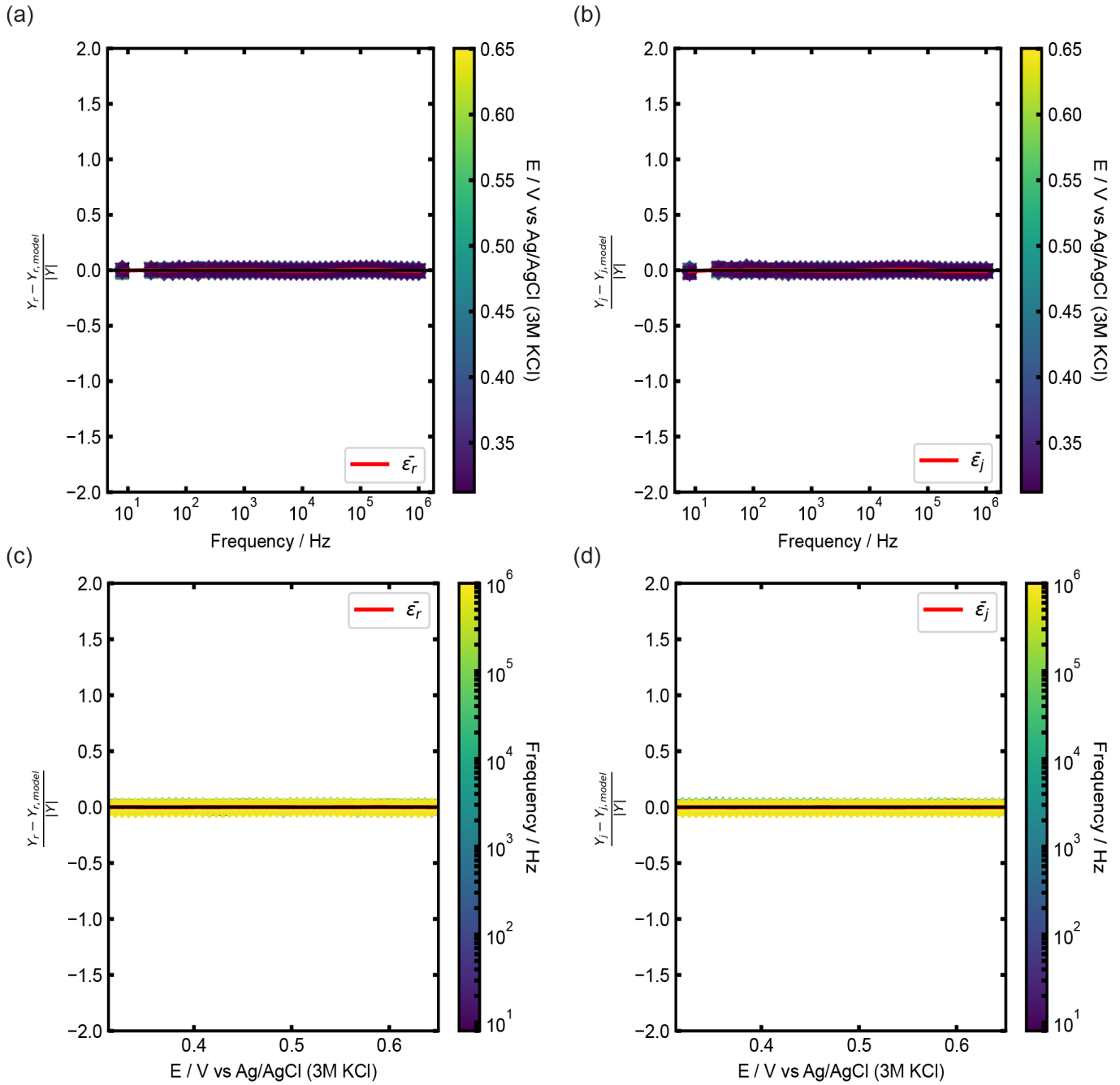


Fig. 7. Residual errors for the spline-fitting plotted as a function of frequency for the (a) real and (b) imaginary parts and as a function of voltage for the (a) real and (b) imaginary parts. The red line represents the mean of the values.

Next, to present a comprehensive analysis of the effect of using the spline method, in Fig. 5 (c) and (d) we show the plots of the resulting parameters as a function of time. Evidently, the spline fitting preserves the dependence between the parameters and allows meaningful trends to be established. However, the trend resulting from the classical-fitting appears much noisier. Moreover the spline fitting yields a lower weighted residual mean square value of 2.81×10^{-5} compared to a value of 14.53 obtained for the classical approach with the chosen

set of initial parameters presented in Table 1. The time it takes to fit the set of 50 spectra is comparable in both cases. On a Windows machine equipped with 32GB RAM and an Intel(R) Core(TM) i7-8750H CPU running at 2.20GHz, the classical-fitting took 7.8 seconds while the spline fitting took 11 seconds. A longer time is needed to determine the optimal number of spline knots; when it is factored in the spline fitting takes 90 seconds. While the computation time of 90 seconds might seem considerable, it's important to note that

this approach obviates the need for selecting an optimal set of initial values. Given this significant advantage, we argue that the computation time is a worthwhile trade-off.

In order to accurately evaluate the residuals from the fit for both methods, the starting values for the classical-fitting were chosen to be closer to the optimal values. The plots of the normalized residuals (i.e normalized by the magnitude of the impedance) as a function of frequency and voltage for the spline-fitting and classical-fitting methods are presented in Fig. 6 and Fig. 7. It can be seen that the normalized residuals of the classical-fitting method show a larger deviation at higher frequencies as shown in Fig. 6 (a) and (b). This is a result of the method failing to fit the high-frequency points whereas the spline-fitting method was able to fit all the points and also resulted in lower residuals (less than two per cent of the magnitude) compared to the classical approach.

IV. CONCLUSION

We have reported a simple and efficient approach for fitting complex impedance data here. This method combines parametric modelling and the use of cubic B-splines. Automatic differentiation was successfully applied to compute the gradient of the cost function with respect to the parameters of the equivalent circuit model. The optimal value of the knots of the spline is chosen using the Akaike information criterion, thus preventing underfitting and overfitting of the parameters. The method is tested on a set of 50 spectra obtained experimentally and compared with the classical approach to fitting multiple spectra as implemented in Impedancepy. The major advantages of the spline-based method are the insensitivity to the choice of starting parameters and the preservation of the dependence of the parameters on the indexing variable. The method is also fast thanks to the JIT compilation provided by the Jax library.

REFERENCES

[1] K. J. Szekeres, S. Vesztergom, M. Ujvári, and G. G. Láng, “Methods for the Determination of Valid Impedance Spectra in Non-stationary Electrochemical Systems: Concepts and Techniques of Practical Importance,” *ChemElectroChem*, vol. 8, no. 7, pp. 1233–1250, 2021. doi: 10.1002/celec.202100093.

[2] D. Aurbach et al., “Common Electroanalytical Behavior of Li Intercalation Processes into Graphite and Transition Metal Oxides,” *J. Electrochem. Soc.*, vol. 145, no. 9, pp. 3024–3034, 1998, doi: 10.1149/1.1838758.

[3] H. M. Cho, W. S. Choi, J. Y. Go, S. E. Bae, and H. C. Shin, “A study on time-dependent low temperature power performance of a lithium-ion battery,” *J. Power Sources*, vol. 198, pp. 273–280, 2012, doi: 10.1016/j.jpowsour.2011.09.111.

[4] Y. M. Choi and S. Il Pyun, “Effects of intercalation-induced stress on lithium transport through porous LiCoO₂ electrode,” *Solid State Ionics*, vol. 99, no. 3–4, pp. 173–183, 1997, doi: 10.1016/s0167-2738(97)00253-1.

[5] C. Erinmwingbovo et al., “Dynamic impedance spectroscopy of LiMn₂O₄ thin films made by multi-layer pulsed laser deposition,” *Electrochim. Acta*, vol. 331, 2020, doi: 10.1016/j.electacta.2019.135385.

[6] R. L. Sacci, F. Seland, and D. A. Harrington, “Dynamic electrochemical impedance spectroscopy, for electrocatalytic reactions,” *Electrochim. Acta*, vol. 131, pp. 13–19, 2014, doi: 10.1016/j.electacta.2014.02.120.

[7] P. Gasper, A. Schiek, K. Smith, Y. Shimonishi, and S. Yoshida, “Predicting battery capacity from impedance at varying temperature and state of charge using machine learning,” *Cell Reports Phys. Sci.*, vol. 3, no. 12, p. 101184, 2022, doi: 10.1016/j.xcrp.2022.101184.

[8] F. Ciucci, “Modeling electrochemical impedance spectroscopy,” *Curr. Opin. Electrochem.*, vol. 13, pp. 132–139, 2019, doi: 10.1016/j.coelec.2018.12.003.

[9] P. Zoltowski, “A new approach to measurement modelling in electrochemical impedance spectroscopy,” *J. Electroanal. Chem.*, vol. 375, no. 1–2, pp. 45–57, 1994, doi: 10.1016/0022-0728(94)13406-5.

[10] A. B. Tesler, D. R. Lewin, S. Baltianski, and Y. Tsur, “Analyzing results of impedance spectroscopy using novel evolutionary programming techniques,” *J. Electroceramics*, vol. 24, no. 4, pp. 245–260, 2010, doi: 10.1007/s10832-009-9565-z.

[11] K. Kobayashi and T. S. Suzuki, “Development of impedance analysis software implementing a support function to find good initial guess using an interactive graphical user interface,” *Electrochemistry*, vol. 88, no. 1, pp. 39–44, 2020, doi: 10.5796/electrochemistry.19-00058.

[12] M. Žic, “Solving CNLS problems by using Levenberg-Marquardt algorithm: A new approach to avoid off-limits values during a fit,” *J. Electroanal. Chem.*, vol. 799, no. March, pp. 242–248, 2017, doi: 10.1016/j.jelechem.2017.06.008.

[13] J. R. Dygas, K. Pietruczuk, W. Bogusz, and F. Krok, “Joint least-squares analysis of a set of impedance spectra,” *Electrochim. Acta*, vol. 47, no. 13–14, pp. 2303–2310, 2002, doi: 10.1016/S0013-4686(02)00078-6.

[14] A. Battistel, G. Du, and F. La Mantia, “On the Analysis of Non-stationary Impedance Spectra,” *Electroanalysis*, vol. 28, no. 10, pp. 2346–2353, 2016, doi: 10.1002/elan.201600260.

[15] M. D. Murbach, B. Gerwe, N. Dawson-Elli, and L. Tsui, “impedance.py: A Python package for electrochemical impedance analysis,” *J. Open Source Softw.*, vol. 5, no. 52, p. 2349, 2020, doi: 10.21105/joss.02349.

[16] C. de Boor, *A Practical Guide to Splines*, Revised ed. New York, NY, USA: Springer-Verlag, 2001.

[17] N. J. Smith et al., “pydata/patsy: v0.5.3,” Zenodo, 2021. [Online]. Available: <https://doi.org/10.5281/zenodo.592075>.

[18] J. Bradbury et al., “JAX: Composable transformations of Python+NumPy programs.” [Software]. Available: <http://github.com/google/jax>. Version 0.3.13, 2018.

[19] M. Blondel et al., “Efficient and Modular Implicit Differentiation,” arXiv preprint arXiv:2105.15183, 2021. Available: <https://arxiv.org/abs/2105.15183>.

[20] P. Virtanen et al., “SciPy 1.0: Fundamental Algorithms for Scientific Computing in Python,” in *Nature Methods*, vol. 17, pp. 261–272, 2020. [Online]. Available: <https://rdocu.be/b08Wh>. doi: 10.1038/s41592-019-0686-2.

[21] R. Chukwu, J. Mugisa, D. Brogioli, and F. La Mantia, “Statistical Analysis of the Measurement Noise in Dynamic Impedance Spectra,” *ChemElectroChem*, vol. 9, no. 14, 2022, doi: 10.1002/celec.202200109.

[22] D. V. Likhachev, “Selecting the right number of knots for B-spline parameterization of the dielectric functions in spectroscopic ellipsometry data analysis,” *Thin Solid Films*, vol. 636, pp. 519–526, 2017, doi: 10.1016/j.tsf.2017.06.056.

[23] T. Mackenzie, “Modelling a Time-dependant Hazard Ratio with Regression Splines,” 1993, [Online]. Available: <https://scholar.google.com/scholar/>

[24] M. Ingdál, R. Johnsen, and D. A. Harrington, “The Akaike information criterion in weighted regression of immittance data,” in *Electrochimica Acta*, vol. 317, pp. 648–653, Sep. 2019. [Online]. Available: <https://doi.org/10.1016/j.electacta.2019.06.030>